A Frequency-domain optofluidic dissolved oxygen sensor with total internal reflection design for in situ monitoring

Bo Xiong, Eric Mahoney, Joe F. Lo, Qiyin Fang*

***Abstract*— Continuous measurements of dissolved oxygen (DO) variation is important in water monitoring and biomedical applications, which require low-cost and low-maintenance sensors capable of automated operation. A frequency-domain optofluidic DO sensor with total internal reflection (TIR) design has been developed based on fluorescence quenching of Ruthenium complex ($Ru(dpp)_3Cl_2$). To minimize artifacts causing drift in fluorescence measurements such as background autofluorescence, photobleaching, optical alignment variation, a low-cost frequency-domain approach is implemented in an optofluidic platform to measure the phase shift between the excitation and emission light. We show that the frequency domain optofluidic DO sensor provides absolute DO concentrations in repeated measurements. TIR design can enhance fluorescence signal in the integrated device and minimize background autofluorescence in the sample, which can subsequently improve overall sensitivity. Furthermore, photobleaching in the samples would be mitigated as the incident light does not enter the microfluidic channel. Our results demonstrate a measurement resolution of 0.2 ppm and response times of less than one minute. In accelerated photobleaching conditions, the long-term drift is shown to be less than ±0.4 ppm. These results suggest the potential of this optofluidic DO sensor as an *in situ* platform for water monitoring and biomedical applications.**

***Index Terms*—Dissolved gas analysis, Fluorescence, Microfluidics, Biomedical monitoring, Environmental monitoring**

I. Introduction

Dissolved oxygen (DO) concentration is an important indicator for water quality. In a stable body of fresh water, the concentration of DO ranges from 8 ppm to 14 ppm and varies in different conditions including temperature [1]. Marine creatures require a DO concentration of at least 5 ppm to survive [1], while anaerobic condition (<1 ppm) promotes the release of pollution from sediments into overlying water [2]. DO monitoring can be used for early warning of algae blooming [3], drink water quality [4] and other contamination events. DO concentration is also monitored and controlled in wastewater treatments [5-6]. By monitoring DO concentration decreasing rate, organic pollution in water can be evaluated using BOD (Biochemical Oxygen Demand) tests [7-8], which are used to forecast the incoming load for wastewater treatment plants to optimize treatment strategy [9-10]. At present, DO is usually manually measured on site (e.g. in river, lake, or water treatment bioreactors) while BOD tests are generally performed in a lab. Automatic and continuous monitoring of DO/BOD values in the waterbody is highly desired.

Monitoring the oxygenation of cells and tissues is also of interest in metabolic imaging applications. The metabolic status and rate of oxygen consumption can be used to assess functional and dysfunctional cells, and to determine cellular responses to treatment for disease or cancers [11-12]. Measurement of embryonic oxygen consumption may also indicate the quality of embryos for applications in In-Vitro Fertilization [13]. Metabolic status of cells has been determined by monitoring the oxygen reduction ratio of electron acceptors in cells using Fluorescence Lifetime Imaging (FLIM) [14-15]. Oxygenation of cells and tissues has been accomplished by measuring the collisional quenching of oxygen sensitive phosphorescent dyes using Phosphorescent Lifetime Imaging (PLIM) which is complementary to FLIM [16].

There are two main requirements for DO monitoring sensors in such applications: (i) automated, continuous and repeated measurement must be performed without manual intervention; and (ii) low maintenance, calibration free, low power consumption, and free of chemical reagent.

Chemical, electrochemical and optical methods have been used in DO sensing. In chemical DO sensing, titration that produces color change has been the standard for accuracy and precision when measuring dissolved oxygen [17]. However, titrimetric procedures consume chemical reagents and require manual lab work. Electrochemical DO sensors typically use Clark electrode which relies on the electrocatalytic reaction of oxygen on platinum [18-19]. Nevertheless, several common drawbacks of electrochemical sensors limit their usage in *in situ* water monitoring, including interferences from other ions, requirements of water flow, frequent calibrations and limited lifetime caused by electrode aging. In contrast, optical DO sensors are based on collisional quenching between oxygen and fluorophores/phosphors in a polymer matrix [20-24]. Optical DO sensors present advantages of no consumable reagent, less interferences from other ions, long working lifetime, and reversable, continuous mode of operation.

In optical DO methods, both fluorescence intensity [20] and lifetime [21] can be used to quantify DO according to Stern-Volmer equation [24]:

$$\frac{I_f^0}{I_f} = \frac{\tau_0}{\tau} = 1 + k_q \tau_0 [Q] \quad (1)$$

where k_q is the quenching constant; $[Q]$ is the concentration of

dissolved oxygen; I_f and τ are fluorescence intensity and fluorescence lifetime without dissolved oxygen; I_f^0 and τ_0 are fluorescence intensity and fluorescence lifetime in the presence of dissolved oxygen, respectively. Time-resolved fluorescence (trF) based approaches are attractive in automated measurements since intensity variations caused by photobleaching, dye leaching, detector drift, laser output fluctuation, change in optical path, etc., have less effect on fluorescence lifetime [21-22, 25-26]. However, current optical DO sensors used in environmental applications are still expensive, large, has high power consumption compared with electrochemical DO sensors.

Frequency-domain method is another way to achieve time-resolved fluorescence measurements with low-cost light sources and detection systems [23-24, 27]. With a sinusoidal excitation light, the fluorescence signal is also modulated but phase shifted relative to the excitation light. Assuming the fluorescence is a single-exponential decay, its lifetime can be estimated from the phase shift between excitation and emission signals at the modulation frequency, as shown in Eq. 1:

$$\phi(f) = \tan^{-1}(2\pi f\tau) \qquad (2)$$

Where f is the modulation frequency; $\phi(f)$ is the relative phase shift; and τ is the fluorescence lifetime.

Recent advances in miniaturized optical and electronic components including lenses, light sources, photo detectors and data acquisition devices enable the instrumentation of portable optical sensors with microfluidic devices. The frequency-domain fluorescence lifetime measurements can be achieved by a low-cost approach which uses a camera with a rolling shutter [28]. Nanotechnologies, such as, core–shell nanoparticles [29] can be used to enhance the change of fluorescence intensity/lifetime in response oxygen concentration. Therefore, a frequency-domain optofluidic device could be a promised approach for DO monitoring in *in situ* applications.

In this paper, we report the development of an optofluidic DO sensor for continuous, repeated in situ DO monitoring. A frequency-domain fluorescence detection method is applied to measure oxygen concentration without the need for calibrations in every measurement and suppress long-term drift. The fluorescence signal is enhanced by a total internal reflection (TIR) design, which minimizes background autofluorescence in the water sample. Photobleaching to the samples could be mitigated as the incident light does not enter the microfluid channel. Such an optofluidic platform would allow automated preprocessing of the sample and enables potential BOD measurements and biomedical applications.

II. Materials and Methods

A. Reagents

Polydimethylsiloxane (PDMS) Sylgard 184 was purchased from Dow Corning (Midland, MI). RuTris (4,7-diphenyl-1,10-phenanthroline) ruthenium (II) dichloride ($Ru(dpp)_3Cl_2$) was purchased from Alfa Aesar (Haverhill, MA). Anhydrous alcohol was purchased from Commercial Alcohols Inc. (Brampton, CA).

B. Sensor Design

As shown in Fig. 1a, the fluidic module of the DO sensor consists four layers: (i) a microfluidic chamber with a cap, (ii) a DO sensitive layer, (iii) a glass slide as substrate, and (iv) a prism. Water flow is confined in the PDMS cap and the total volume of the water channel is about 192 ul (L×W×H: 16×8×1.5 mm). The DO sensitive layer consists of PDMS and $Ru(dpp)_3Cl_2$. An excitation beam is coupled into the DO sensitive layer with an incident angle θ, as shown in Fig. 1a. The wedged angle of the prism is the same as the incident angle θ to make sure the excitation beam is perpendicular to the entry surface of the prism.

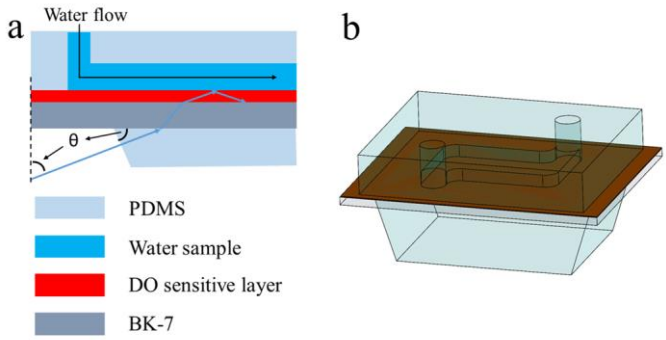

Fig. 1. (a) Side and (b) 3D schematic view of the DO sensor

C. Chip Fabrication

$Ru(dpp)_3Cl_2$ is dissolved in anhydrous alcohol (1:10 w/w) and then mixed in PDMS which is mixed with a 10:1 ratio of base: curing agent. The weight ratio of $Ru(dpp)_3Cl_2$ to PDMS is 1:200. Next, the complex was coated on the microscope slide by spin coating at 3000 rpm for 60 s. This process produced a DO sensitive layer of 15 μm in thickness. Finally, the DO sensitive layer is cured by heating at 90°C for 12 hours.

D. Simulation and Optimization

The incident angle θ (defined in Fig. 1a) is optimized by ray tracing simulation in Zemax™. Two design configurations of sensors are used in the simulation: (a) the proposed design with a prism and (b) a design without a prism, as shown in Fig. 2a and Fig. 2b. Parallel excitation beams with different incident angles were induced and the fluorescence intensities generated by the DO sensitive layer were calculated using the ray tracing model.

As shown in Fig. 2c, the fluorescence intensity increases by 7 times at 80 degree in the proposed design. When θ is larger than 70 degrees, total internal reflection of the excitation beam takes place at the surface between the DO sensitive layer and the sample. As a result, the optical path of the excitation light within the DO sensitive layer increases, leading to an increased absorption of excitation light. Conversely, in the design without the prism (Fig. 2b), when the incident angle is larger than 60 degrees, the high reflection rate of the excitation beam at the air/glass interface and the glass/PDMS interface results in the reduction of fluorescence intensity.

Ray tracing simulation is performed to demonstrate that the

autofluorescence generated in the water sample can be reduced using the proposed design with a prism. Assuming that fluorophores are present in the water sample, excitation beams with different incident angles θ were induced and fluorescence intensities generated by the water sample were calculated. When θ is larger than 70 degrees, TIR limits the excitation of bulk water. As a result, the fluorescence from water channel is reduced as shown in the blue curve in the Fig. 2d.

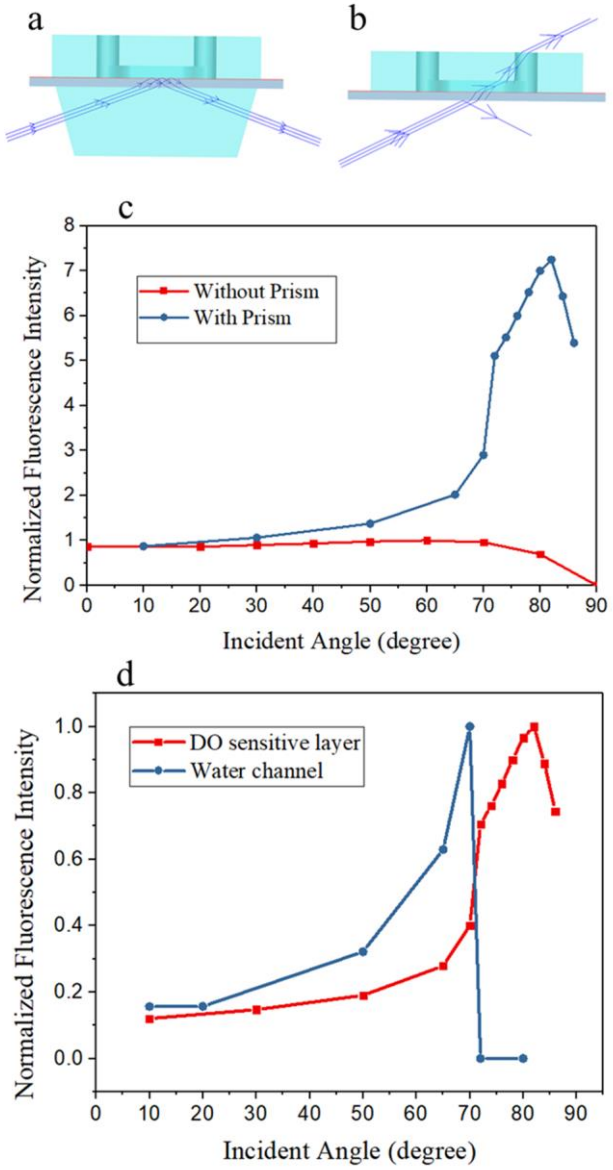

Fig. 2. Ray tracing model of (a) proposed design with prism coupling and (b) control design without prism coupling. (c) Normalized fluorescence intensity based on the ray tracing simulation of the two designs. The fluorescence intensity is normalized by the maximum intensity in the control group (i.e. the 60 degree point). (d) Normalized fluorescence intensity generated in the DO sensitive layer and fluidic channel in the TIR design. Refraction indexes used in the simulation are water:1.33, air:1.01, PDMS:1.416 and glass slide: 1.51.

Therefore, θ is chosen to be 80 degree in the DO sensor to enhance the fluorescence and mitigate the unintended autofluorescence in the water sample. These simulation results indicate that fluorescence generated by DO sensitive layer can be enhanced by using the TIR design. At the same time, the background autofluorescence from the water sample can be reduced.

III. Experimental Setup

Following the design optimization in the simulation, a customized frequency domain DO setup was built (Fig. 3). A 450 nm laser (450, Wuhan Besram Technology Inc, Wuhan, China) is modulated by a square signal with a frequency of 160 kHz and the output power after the pin hole is 15.5 mW. The excitation beam is coupled into the DO sensor with an incident angle of 80 degrees. The emitted fluorescent light is coupled into a photoelectric detector (APD 120A, Thorlabs, Newton, NJ) with a relay assemble consists of two aspherical lenses (EFL = 20 mm, ACL2520U-A, Thorlabs). An emission filter (BrightLine® FF01-609/181-25, Semrock, Rochester, NY) with a center wavelength of 609 nm and a bandwidth of 180 nm is used to block the excitation light.

The square modulation signal from a waveform generator and the distorted square signal from the photoelectric detector are sent to a digitizer (PicoScope, Pico Technology, Cambridgeshire, UK). Then resulting signal at frequency of 160kHz is decomposed from square waves and distorted square waves with Fast Fourier Transform. The phase shift between the two sinusoidal signals were measured to quantify the DO concentration in the water sample. The water samples were prepared by bubbling oxygen or nitrogen through the drinking water to get a certain DO concentration. It was then delivered into the water channel with a syringe pump at 50 µl/s. Before delivery, the DO concentration in the sample are measured with a commercial DO sensor (ExStik® DO600, Extech Instruments , Waltham, MA). All experiments are performed at room temperature. This setup can be miniaturized in a low-cost and portable design with customized printed circuit boards and embedded software in the future.

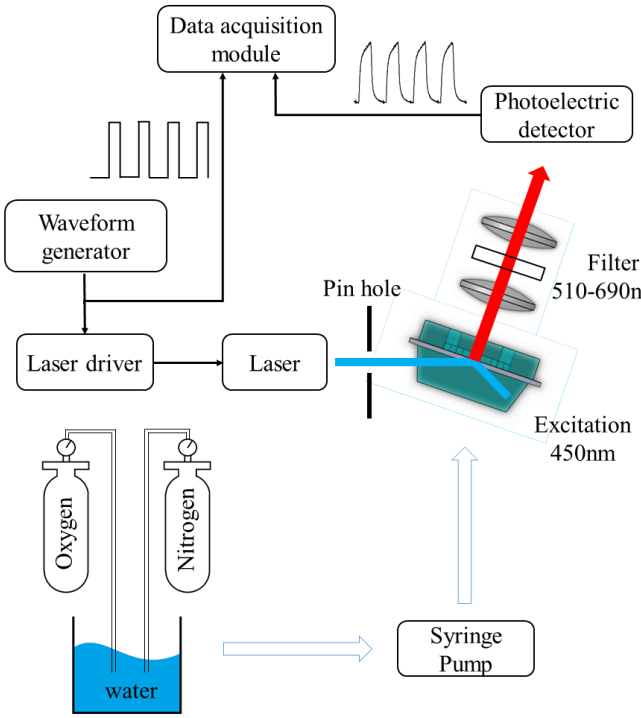

Fig. 3. Customized frequency domain DO setup

IV. Results and Discussion

A. Enhancement of Fluorescence Signal

To verify to the enhancement of fluorescence intensity by the TIR design and prism coupling, two excitation configurations are compared: 1) excitation without meeting the TIR condition, i.e. the excitation beam was coupled from the bottom chip at the incident angle of 45 degrees; and 2) excitation with the TIR at the optimum excitation angle of 80 degrees. The fluorescence intensity is measured with a power meter. Then two excitation configurations are used sequentially, and the measurements were repeated 8 times, as shown in the Fig. 4a. The results shown in Fig. 4b indicate that the collected fluorescence intensity is increased by 2.7 times by using prism coupling with an incident angle of 80 degrees. The enhancement factor is lower than that in the simulation, which may be the result of scattering in the DO sensitive layer. The enhancement of fluorescence intensity contributes to a better SNR (signal noise ratio) of photodetector output which is a key factor that affects the limit of detection. Alternatively, lower power lasers and low-cost photo detectors can be used to miniaturize the overall system size with reduced cost. These improvements will enable potential integration of all component on a single detection chip in the future.

B. DO Sensing Performance

To evaluate the performance of DO sensor, sensing resolution, repeatability and response time are tested. The DO sensor is calibrated against the commercial DO sensor reading using water samples at seven different DO concentrations: 12.80 ppm, 9.90 ppm, 7.65 ppm, 5.65 ppm, 4.05 ppm, 1.71 ppm, and 0.10 ppm. For each sample, 6 separate measurements were taken respectively. For each one measurement, 256 cycles of a square signal are sent to a laser driver, and the total exposure time is 0.8 ms. The phase shift caused by instrumentation response was measured with a reference microfluidic chip without the Ru complex in the DO sensitive layer. As shown in Fig.5, the phase shift decreases as the DO concentration increases. Then a calibration curve is obtained using linear interpolation between the calibration points.

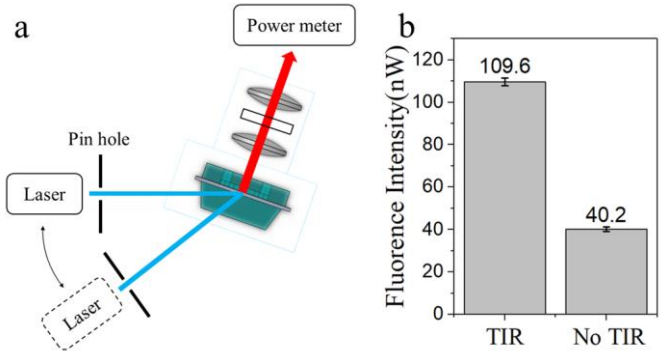

Fig. 4. Comparison of fluorescence intensity between two excitation configurations: TIR and no TIR. (a) experimental configurations. Laser and pinhole are moved to switch excitation configurations. (b) experimental results. The error bar is standard deviation over 4 repeated measurements. This error is caused by slight alignment difference among measurements.

The resolution of DO measurements at each point can be obtained using the production of standard deviation (SD) of the phase shift among 6 measurements and the slope of the oxygen concentration-phase shift curve. As a result, a measurement resolution of 0.19 ppm is obtained at 9.90 ppm where the SD of measured DO is largest. The standard error for SD estimation is 0.03ppm. This measurement resolution is comparable to some commercially available optical DO sensors [30] with a resolution of 0.1ppm, which are commonly used in environmental and biological applications. There are two approaches can be used to improve the DO resolution of proposed device when better a measurement resolution is required: (i) using moving average with a long time period (ii) using a fluorophore with higher oxygen sensitivity, such as, Pt complex [29].

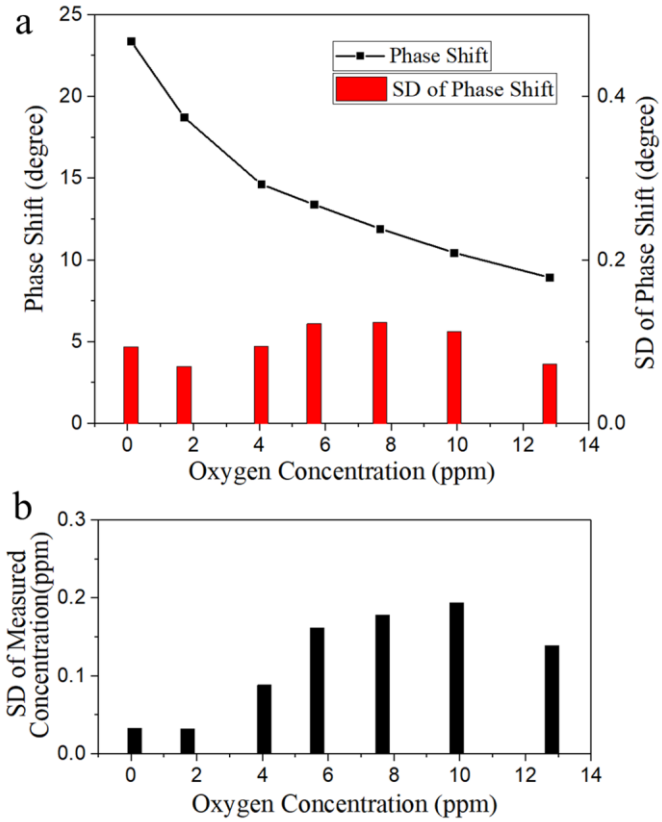

Fig. 5. (a) A calibration curve is obtained to predict the DO concentration of unknown phase shift. Linear interpolation is used between 7 calibration points. The standard deviation of the phase shift over 6 repeated measurements is shown at each calibration point. (b) The resolution of measured DO concentrations.

The measurement repeatability was characterized using samples at two different oxygen concentration: 0.10 ppm and 7.59 ppm. The samples were prepared at the two oxygen concentrations, which were verified by the commercial DO sensor. Then they were measured sequentially 150 seconds after each water sample injection. The measurements were repeated 8 times. The measurement results indicate an excellent repeatability of the DO sensing: $\pm$ 0.2 ppm at 7.59 ppm and $\pm$0.05 ppm at 0.10 ppm, as shown in Fig.6.

The response time of the frequency domain DO device was

characterized. The response time is defined as 90% of the response (or recovery) time when switching between two samples at two different oxygen concentration: 0.10 ppm and 7.59 ppm. As shown in Fig. 7, the water switch occurs after 8 seconds measurements begin, and there is a lag time before the measured DO concentration become stable. The main contributor of this lag time is the oxygen diffusion between water and the PDMS membrane until equilibrium is reached. Therefore, a thinner DO sensitive layer is helpful to reduce response time. However, a thinner DO sensitive layer may have a negative effect on DO sensitivity due to weak fluorescence intensity [20]. Currently, this frequency domain DO device has a response time of 23 s when switching from deoxygenated water to oxygenated water and 40 s when switching from oxygenated water to deoxygenated water. These results show that the frequency domain DO device can response to oxygen variation in less than one minute which is fast enough for most of water monitoring applications [31].

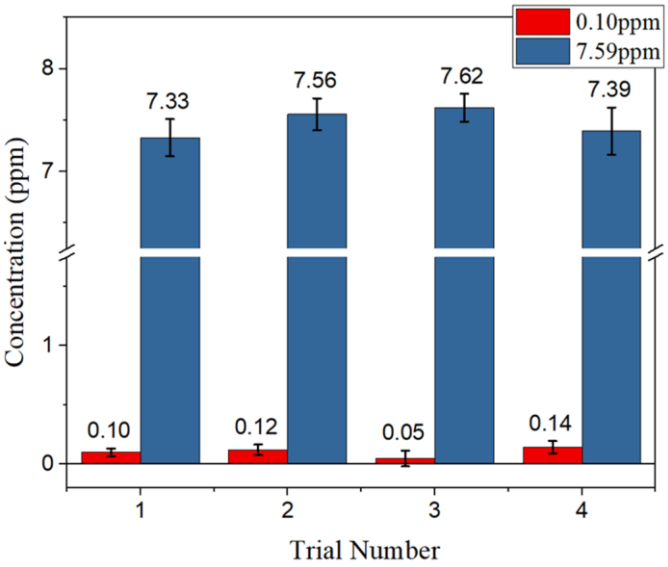

Fig. 6. Repeatability results of DO measurements using two samples. Red: using water sample with 0.10 ppm DO. Blue: using water sample with 7.59 ppm DO. The error bars are calculated from the standard deviation (SD) of 6 measurements.

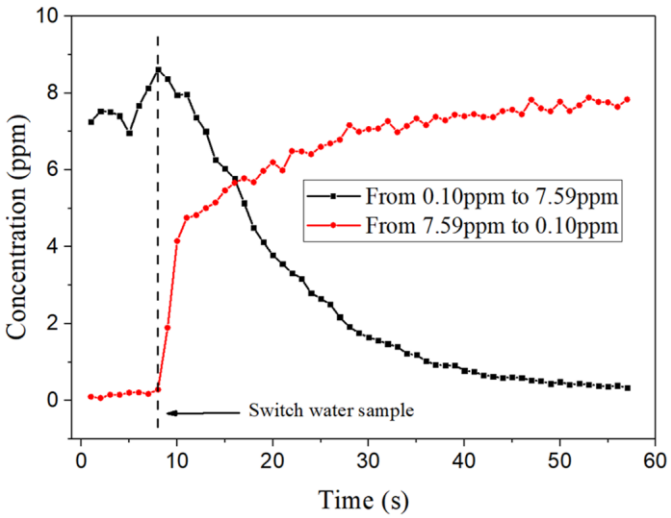

Fig. 7. Response curves of frequency domain DO device when switching between two samples at two different oxygen concentration: Red line shows the measured DO when switching from 0.10 ppm sample to 7.59 ppm sample. Black line shows the measured DO when switching from 7.59 ppm sample to 0.10 ppm sample. DO concentration is measured with a sampling rate of 1 Hz.

C. *Accelerated photobleaching test*

An accelerated photobleaching test is performed to estimate the photobleaching effect on the frequency domain optofluidic platform. A 128 s exposure was used to induce photobleaching, which corresponds to 80,000 DO measurements (80k = 128 * 160 k / 256). Water sample with a DO concentration of 8.38 ppm is injected and the DO concentration is monitored with the optofluidic platform. Assuming that the DO measurement is taken 6 times per hour in a long-term monitoring setting, this 128 s exposure corresponds to 18 months of regular use. As shown in Fig. 8, the measured fluorescence intensity decreases about 20% during 128 s. According to Equation (1), the decrease of fluorescence intensity can result in a drift when DO is quantified by static fluorescence intensity measurements. When the frequency domain method is used, fluctuation of the measured DO concentration is about ± 0.4 ppm and the drift is suppressed dramatically. These results show that the proposed frequency-domain optofluidic platform is suitable for long-term monitoring because frequency-domain methods could be less sensitive to photobleaching or other variations of fluorescence intensity.

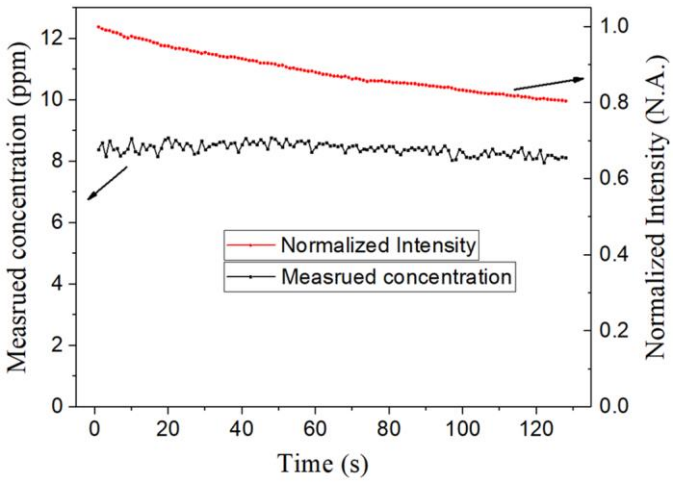

Fig. 8. Accelerated photobleaching test of frequency domain DO device. Red line and black line show the normalized fluorescence intensity and measured DO concentration over 128 s, respectively. DO concentration is measured with a sampling rate of 1 Hz.

V. Conclusion

In summary, a frequency domain optofluidic dissolved oxygen sensor with a TIR enhancement is developed. The DO sensor has a resolution of 0.2 ppm over a concentration range of 0.1 ppm to 12.8 ppm. This platform is suitable for long-term monitoring owing to the frequency-domain method and an efficient TIR design. The use of microfluidic platforms allows preprocessing of the sample, such as, temperature control, adding reagent, etc. Thus, cell culture BOD monitoring could be enabled in the optofluidic platform.

TIR design increased fluorescence signal and minimized background autofluorescence from fluorophore in the sample fluidic channel since the excitation is confined within the

non-fluidic layers. Consequently, enhanced sensitivity could enable in situ monitoring of oxygen concentrations in biological samples as well as oxygen consumption rates. When combined with the TIR design, measurements can be conducted without optically damaging the cells themselves or photobleaching intrinsic fluorophores as the excitation light does not enter the fluid channel. The design could have applications in cell culture monitoring and embryo assessment [11-12, 32].

A low-cost luminescent lifetime imaging method that developed recently can be potentially applied to this design [14]. FLIM measurement of fluorescent films or foils have been explored as a method for monitoring extracellular oxygen as an indication of the oxygenation and oxygen consumption of cells and tissues [12, 31]. Although these films are not able to visualize the distribution of oxygen within individual cells, they are easy to fabricate, low-cost, and do not negatively impact cell viability as the indicator does not need to be delivered into the cells [11]. Fabricating fluid channels or micro-wells above oxygen sensitive phosphorescent films enables monitoring the oxygenation of fluids being delivered to cell cultures or monitoring the microenvironment of individual wells [32].

ACKNOWLEDGMENT

This project is supported in part by the Natural Science and Engineering Research Council (NSERC) of Canada, the Province of Ontario through an Ontario Research Fund (ORF-RE). QF held the Canada Research Chair in Biophotonics. BX holds a Chinese Scholarship Council PhD scholarship and EM held an Ontario Graduate Scholarship and a McMaster Faculty of Engineering Dean's PhD Excellence Scholarship.

REFERENCES

[1] U.S. Environmental Protection Agency, "Chapter 9: Dissolved oxygen and biological oxygen demand," in Voluntary Estuary Monitoring Manual: A Methods Manual, 2nd ed. Washington, DC, USA: U.S. Environmental Protection Agency, Office of Wetlands Oceans and Watersheds, Mar. 2006.

[2] T. Zoumis, A. Schmid, L. Grigorova, and W. Calmano, "Contaminants in sediments: remobilisation and demobilisation." Science of the total environment, vol. 266, no. 1-3, pp. 195-202, 2001.

[3] J. H. W. Lee, I. J. Hodgkiss, K. T. M. Wong, and I. H. Y. Lam, "Real time observations of coastal algal blooms by an early warning system." Estuarine, Coastal and Shelf Science, vol. 65, no. 1-2, pp. 172-190, 2005.

[4] D. Hou et al., "An early warning and control system for urban, drinking water quality protection: China's experience." Environmental Science and Pollution Research, vol. 20, no. 7, pp. 4496-4508, 2013.

[5] J.M. Garrido et al., "Influence of dissolved oxygen concentration on nitrite accumulation in a biofilm airlift suspension reactor." Biotechnology and bioengineering, vol. 53, no. 2, pp. 168-178, 1997.

[6] L. Åmand and B. Carlsson. "The optimal dissolved oxygen profile in a nitrifying activated sludge process–comparisons with ammonium feedback control." Water Science and Technology, vol. 68, no. 3, pp. 641-649, 2013.

[7] D. J. Barker et al., "Characterisation of soluble residual chemical oxygen demand (COD) in anaerobic wastewater treatment effluents." Water Research, vol. 33, no. 11, pp. 2499-2501, 1999.

[8] S. Jouanneau et al., "Methods for assessing biochemical oxygen demand (BOD): A review." Water research, vol. 49, pp. 62-82, 2014.

[9] M. Kim et al., "Evaluation of the k-nearest neighbor method for forecasting the influent characteristics of wastewater treatment plant." Frontiers of Environmental Science & Engineering, vol. 10, no. 2, pp. 299-310, 2016.

[10] A. Kusiak, A. Verma and X. Wei. "A data-mining approach to predict influent quality." Environmental monitoring and assessment, vol. 185, no. 3, pp. 2197-2210, 2013.

[11] D. B. Papkovsky and R. I. Dmitriev, "Imaging of oxygen and hypoxia in cell and tissue samples," Cell. Mol. Life Sci., vol. 75, no. 16, pp. 2963–2980, Aug. 2018.

[12] Y. Zhao et al., "A platinum-porphine/poly(perfluoroether) film oxygen tension sensor for noninvasive local monitoring of cellular oxygen metabolism using phosphorescence lifetime imaging," Sensors Actuators B Chem., vol. 269, pp. 88–95, Sep. 2018.

[13] T. Sanchez et al., "Combined noninvasive metabolic and spindle imaging as potential tools for embryo and oocyte assessment," Hum. Reprod., vol. 34, no. 12, pp. 2349–2361, Dec. 2019.

[14] P. S. Chelushkin and S. P. Tunik, "Phosphorescence Lifetime Imaging (PLIM): State of the Art and Perspectives," in Springer Series in Chemical Physics, vol. 119, no. January, Springer International Publishing, 2019, pp. 109–128.

[15] J. Hou et al., "Correlating two-photon excited fluorescence imaging of breast cancer cellular redox state with seahorse flux analysis of normalized cellular oxygen consumption," J. Biomed. Opt., vol. 21, no. 6, p. 060503, Jun. 2016.

[16] K. Jahn, V. Buschmann, and C. Hille, "Simultaneous Fluorescence and Phosphorescence Lifetime Imaging Microscopy in Living Cells," Sci. Rep., vol. 5, no. 1, p. 14334, Nov. 2015.

[17] J. H. Carpenter, "The accuracy of the Winkler method for dissolved oxygen analysis." Limnology and Oceanography, vol. 10, no. 1, pp. 135-140, 1965.

[18] L. C. Clark and C. Lyons, "Electrode systems for continuous monitoring in cardiovascular surgery." Annals of the New York Academy of sciences, vol. 102, no. 1, pp. 29-45, 1962.

[19] L. Hsu et al., "Development of a low-cost hemin-based dissolved oxygen sensor with anti-biofouling coating for water monitoring." IEEE Sensors Journal, vol. 14, no. 10, pp. 3400-3407, 2014.

[20] E. J. Mahoney et al., "Optofluidic Dissolved Oxygen Sensing with Sensitivity Enhancement Through Multiple Reflections." IEEE Sensors Journal, vol. 19, no. 22, pp. 10452-10460, 2019.

[21] M. Quaranta, S. M. Borisov and I. Klimant, "Indicators for optical oxygen sensors." Bioanalytical Reviews, vol. 4, no. 2-4, pp. 115-157, 2012.

[22] K. J. Morris et al., "Luminescence lifetime standards for the nanosecond to microsecond range and oxygen quenching of ruthenium (II) complexes." Analytical chemistry, vol. 79, no. 24, pp. 9310-9314, 2007.

[23] S. B. Bambot et al., " Phase fluorometric sterilizable optical oxygen sensor," Biotechnology and Bioengineering, vol 43 (11), pp. 1139-1145, 1994.

[24] C. S. Chu, Y. L. Lo, T. W. Sung, "Review on recent developments of fluorescent oxygen and carbon dioxide optical fiber sensors." Photonic Sensors, vol 1, no. 3, pp. 234-250, 2011.

[25] C. McDonagh et al., "Phase fluorometric dissolved oxygen sensor." Sensors and Actuators B: Chemical, vol. 71, no. 1-3, pp. 124-130, 2001.

[26] S. A. Yeh, M. S. Patterson, J. E. Hayward and Q. Fang, "Time-resolved fluorescence in photodynamic therapy." Photonics, vol. 1, no. 4, pp. 530-564, 2014.

[27] R. Liu et al., "Compact, non-invasive frequency domain lifetime differentiation of collagens and elastin." Sensors and Actuators B: Chemical, vol. 219, pp. 283-293, 2010.

[28] B. Xiong and Q. Fang, "Luminescence lifetime imaging using cellphone camera with electronic rolling shutter." Optics letter, vol. 45, no. 1, pp. 81-84, 2020.

[29] C. S. Chu, Y. L. Lo and T. W. Sung. "Enhanced oxygen sensing properties of Pt (II) complex and dye entrapped core–shell silica nanoparticles embedded in sol–gel matrix." Talanta, vol. 82, no. 3, pp. 1044-1051, 2010.

[30] https://www.ysi.com/pro20 (2020).

[31] J. F. Lo et al., "Islet preconditioning via multimodal microfluidic modulation of intermittent hypoxia." Analytical chemistry, vol. 84, no. 4, pp. 1987-1993, 2012.

[32] F. Zhu, D. Baker, J. Skommer, M. Sewell, and D. Wlodkowic, "Lab-on-a-chip technology for a non-invasive and real-time visualisation of metabolic activities in larval vertebrates," in Bio-MEMS and Medical Microdevices II, 2015, vol. 9518, no. June 2015, p. 951813.

Bo Xiong received the B.Sc. and M.Sc. degrees in precision machining and instrumentation from Tianjin University in 2013 and 2016, respectively. He is currently pursuing the Ph.D. degree in biomedical engineering with McMaster University. His research interests include the development of advanced sensors for environmental monitoring and point of care diagnostic applications

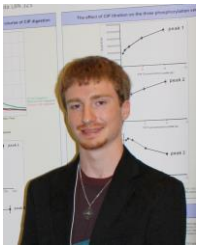

Eric James Mahoney received the B.Tech. (Hons.) degree in biotechnology from McMaster University, Hamilton, ON, Canada, in 2014, where he is currently pursuing the Ph.D. degree in biomedical engineering. His research interests include the field of biophotonics and the development of remote monitoring devices for water quality and point of care diagnostic applications

Joe F. Lo received his BSc degree in Biomedical Engineering from the University of Berkeley and his PhD in Biomedical Engineering from the University of Southern California. He is currently an Associated Professor in the Department of Mechanical Engineering at the University of Michigan, Dearborn. His research interests include microfluidics and MEMS based sensing and imaging device technologies.

Qiyin Fang is a Professor of Engineering Physics and Biomedical Engineering at McMaster University. Dr. Fang received his BSc in Physics from Nankai University and his MASc in Applied Physics and PhD in Biomedical Physics from East Carolina University (Greenville, NC). Prior to his current position at McMaster, Dr. Fang was with the Minimally Invasive Surgical Technology Institute of Cedars-Sinai Medical Center, Los Angeles. Dr. Fang's current research interests include optical spectroscopy and imaging for minimally invasive diagnosis and guided therapy, miniaturized sensors and imaging systems, advanced optical microscopy, and smart sensing systems for aging-in-place and environmental applications. He is a Fellow of SPIE and the Canada Research Chair in Biophotonics.